

Theoretical estimate of the half-life for the radioactive ^{134}Cs and ^{135}Cs in astrophysical scenarios

Simone Taioli*

European Centre for Theoretical Studies in Nuclear Physics and Related Areas (ECT-FBK)
Trento Institute for Fundamental Physics and Applications (TIFPA-INFN), Trento, Italy and
Peter the Great St.Petersburg Polytechnic University, Russia*

Diego Vescovi

Goethe University Frankfurt, Germany

Maurizio Busso, Sara Palmerini

*Department of Physics and Geology, University of Perugia, Italy and
INFN, Sezione di Perugia, Italy*

Sergio Cristallo

*INAF, Osservatorio Astronomico d'Abruzzo, Teramo, Italy and
INFN, Sezione di Perugia, Italy*

Alberto Mengoni

*European Organization for Nuclear Research (CERN), Geneva, Switzerland
Dipartimento Fusione e Tecnologie per la Sicurezza Nucleare, ENEA, Bologna, Italy and
INFN, Sezione di Bologna, Italy*

Stefano Simonucci[†]

*School of Science and Technology, University of Camerino, Italy and
INFN, Sezione di Perugia, Italy*

(Dated: September 30, 2021)

We analyze the $^{134}_{55}\text{Cs} \rightarrow ^{134}_{56}\text{Ba}$ and $^{135}_{55}\text{Cs} \rightarrow ^{135}_{56}\text{Ba}$ β^- decays, which are crucial production channels for Ba isotopes in Asymptotic Giant Branch (AGB) stars. We reckon, from relativistic quantum mechanics, the effects of multichannel scattering onto weak decays, including nuclear and electronic excited states populated above $\simeq 10$ keV, for both parent and daughter nuclei. We find a significant increase (by more than a factor 3 for ^{134}Cs) of the half-lives with respect to previous recommendations [1, 2], and we discuss our method in view of these last calculations based on general systematics. The major impact on half-lives comes from nuclear excited state decays, while including electronic temperatures yields a $\approx 20\%$ increase, at energies typical of low- and intermediate-mass AGB stars ($M \lesssim 8M_{\odot}$). Our predictions strongly modify branching ratios along the s -process path, and allow nucleosynthesis models to account well for the isotopic admixtures of Ba in presolar SiC grains.

Keywords: Electronic and nuclear excited states; β decay; many-body correlation; AGB stars; s -process

Our understanding of the cosmic chemical abundances is closely linked to the measurement or modelling of weak nuclear reaction rates in hot stellar plasma, whose accurate assessment still represents a bottleneck for nuclear astrophysics.

On the experimental side, recent space-born and ground-based spectroscopic observations provide precise abundances in Galaxies at different redshift and ages. Moreover, new scenarios to unravel heavy-element nucleosynthesis in stars were also opened by the analysis of presolar grains [3, 4] formed in the winds of super-

novae, novae and red giants, and trapped in pristine meteorites. Presolar stardust offers a view on the isotopic admixture of heavy elements, readily translated into precise constraints to stellar processes [5]. Unfortunately, experiments reproducing astrophysical conditions in ionized plasmas to measure decay rates are still in their infancy [6, 7].

Thus, the upgrading of evolution and nucleosynthesis models to account for observations must still rely on simulations, most importantly by calculating nuclear physics inputs of stellar reaction rates with increased accuracy

[8]. However, there is a dearth of computational studies of decay processes in astrophysical scenarios from first-principles [9, 10].

One element requiring such studies is barium, which in AGB stars depends solely on *slow(s)* *n*-captures. Starting at stable ^{133}Cs , branching points are found, where further *n*-captures compete with β -decays at ^{134}Cs , such as the $^{134}\text{Cs}(J^\pi = 4^+) \rightarrow ^{134}_{56}\text{Ba}(J^\pi = 4^+) + e^- + \bar{\nu}$ allowed transition, and at ^{135}Cs , in a delicate balance that must yield production of 100% of *s*-only ^{134}Ba and ^{136}Ba . In particular, $^{134}\text{Cs} \rightarrow ^{134}\text{Ba}$ decay (half-life $\simeq 2.0652$ y) is characterized by a *Q*-value (2058.7 keV [11]) large enough to accommodate Cs high-lying nuclear excited states (e.g. 5^+ at 11.2442 keV and 3^+ at 60 keV above the ground state (GS)). The emergence of ^{134}Cs short-lived nuclear excited states, possibly populated at high temperature, and the decay to ^{134}Ba isomers (such as $4^+, 3^+$) may dramatically affect this transition owing to their different forbiddance. Furthermore, despite these transitions are essentially quark-level processes, they strongly depend also on extra-nuclear factors, such as temperature and electron density, significantly varying in the layers of evolved stars outside the degenerate core. Indeed, these parameters may affect the ionization degree of the atomic systems where the decay occurs, which in turn modifies the discrete-to-continuum transition ratio [9, 10, 12]. Along the path of the *s*-process through Cs and Ba isotopes, the *n*-capture on ^{134}Cs feeds the longer-lived ^{135}Cs , which eventually β decays to ^{135}Ba via a 2nd forbidden unique transition $\text{Cs}(7/2^+) \rightarrow \text{Ba}(3/2^+)$, whose half-life is 2.3×10^6 y with a GS-GS *Q*-value of 268.7 keV [13]). The inclusion of several nuclear excited states of the parent ^{135}Cs nucleus (notably the $5/2^+$ states at 249.767 and 408.026 keV above the GS, respectively), as well as the population of electronic excited levels, may affect significantly also this total rate at high temperature.

In this work, we develop a fully relativistic quantum mechanical framework to compute the temperature and density dependence of the β decay half-life of the ^{134}Cs and ^{135}Cs isotopes, by considering both the electronic and nuclear excited state population dynamics. We show that the inclusion of these degrees of freedom (DOF) acts concurrently to lower the relevant Cs isotopes half-lives, even by several orders of magnitude, with respect to laboratory conditions. In order to determine the weak decay rates, we use a mean-field approximation to the internuclear and interelectronic interactions, which proves accurate in reproducing the terrestrial observables [14]. Our suggestions strongly affect previous *s*-process predictions on Cs and Ba isotopes using β -decay half-lives by [1, 2]. In this

respect, we apply our new rates to revise recent models aiming to explain the peculiar ratios of Ba isotopes in presolar SiC grains [5], finding remarkable reconciliation of theory and observations.

In the traditional approach, β decay spectra of allowed and forbidden transitions are calculated by using an analytical expression of the rate [15] where several factors appear, which account for the nuclear and phase-space structure, and for the atomic exchange.

At variance, our approach is based on the first-principle calculation of the total QED Hamiltonian of the system, written as a sum of the internuclear interaction, of the interelectronic repulsive force, and of the weak decay. For a detailed discussion on our method we refer to Supplemental Material (SM), here we sketch the pivotal points. Within our framework, the evaluation of the transition operator is factorized into the product of leptonic and hadronic currents [14]. We also require that the latter term is separable into neutron and proton field operators, which means essentially that the decaying neutron acts as a particle uncorrelated to the *core* of the remaining nucleons. Such core, which couples only geometrically so as to recover the experimental total angular momentum of the parent reactant is approximated by a linear combination of angular momentum wavefunctions. However, this is not a limiting factor: for our method is systematically improvable by using more sophisticated many-body methods [16]. Furthermore, one can safely assume that the leptonic current can be written as a product of the neutrino and electron quantum field operators. The hadronic and leptonic currents are both reckoned by the self-consistent numerical solution of the Dirac-Hartree-Fock equation (DHF) within a mean-field approximation. In this work, protons and neutrons are interacting via a semi-empirical relativistic Wood-Saxon (WS) potential, while the electron-electron Coulomb repulsion is modelled via a local density approximation (LDA) to the electron gas ($V_{ex} \propto \rho(r)^{1/3}$) [17, 18]. Electrons, in particular, populate the energy levels according to a Fermi-Dirac distribution, where the chemical potential is assessed by assuming that they behave as an ideal Fermi gas in a box with a relativistic energy-momentum dispersion at all temperatures. The non-orthogonality between the bound initial and final orbitals, and the possible presence of shake-up and shake-off are also taken into account in the calculation of the continuum electron wavefunction. At very high temperature, we included positron formation, enforcing the overall neutrality of the plasma at all proton densities to model different astrophysical scenarios (see Table

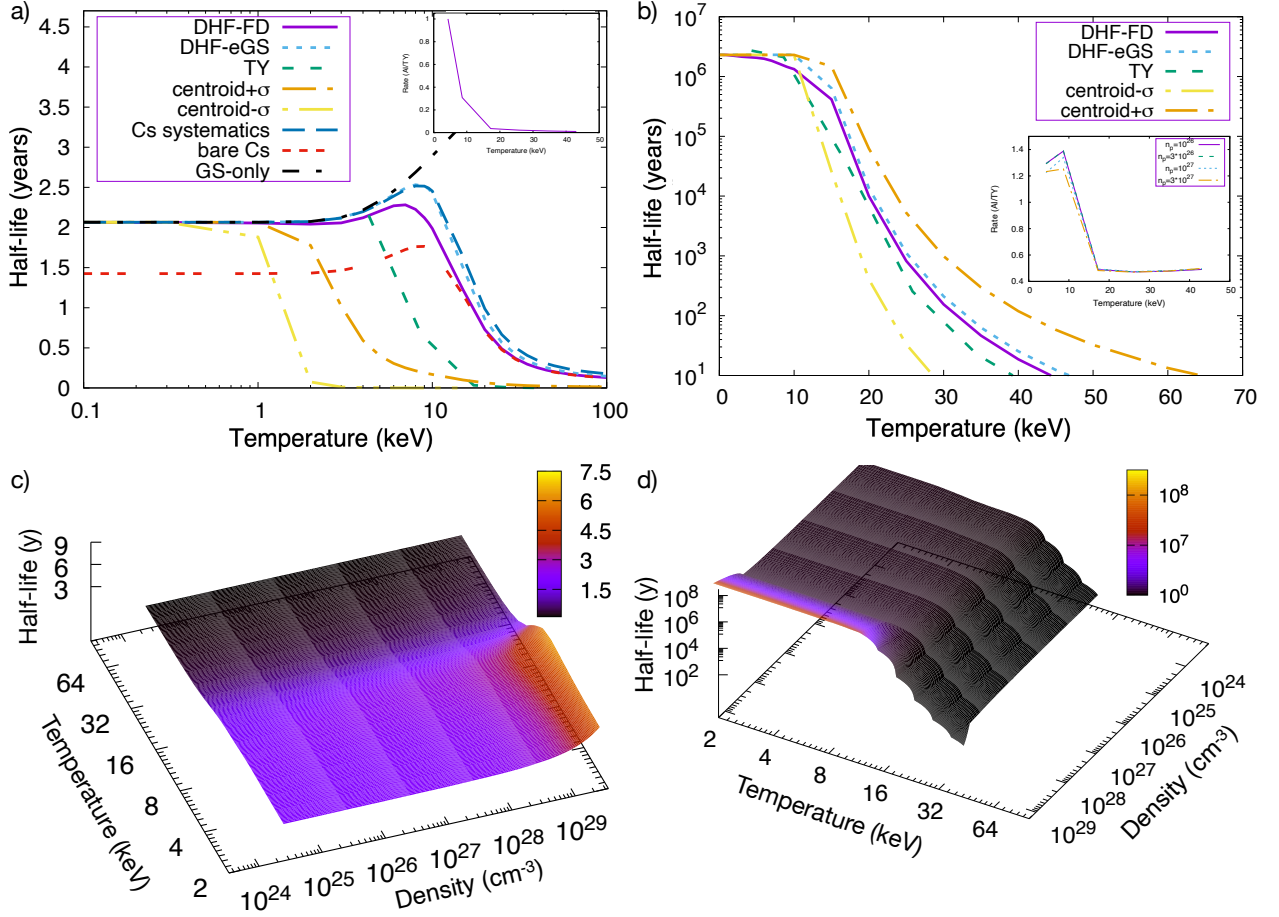


Figure 1. Half-life of ^{134}Cs (a) and of ^{135}Cs (b) vs. temperature (violet line) from our DHF calculations for $n_p = 10^{26} \text{ cm}^{-3}$, including the (a) $4^+, 5^+, 3^+$ ^{134}Cs and (b) $5/2^+, 5/2^+$ ^{135}Cs nuclear states as well as the electronic DOF. In cyan (DHF-eGS) half-life is computed with the electrons clamped in their GS. Orange and yellow lines report the maximum (centroid+ σ) and minimum (centroid- σ) values obtained using the $\log(ft)$ of the general systematics, while in the blue line (Cs systematics) we used the centroid of the specific ^{134}Cs systematics (which do not exist for ^{135}Cs). Green lines show the previous estimates by TY [1, 2]. In panel a) we also show (red line) the half-life for a completely ionized ^{134}Cs (bare Cs) and the nuclear GS to GS decay half-life (black line, GS-only). The trend is the same for ^{135}Cs (not shown). Insets of a) and b) give the ratios between our ab-initio β decay rates (AI) and those by TY [1, 2] for $n_p = 10^{26} \text{ cm}^{-3}$. Panels c) and d) display ^{134}Cs and ^{135}Cs half-lives according to our model, including both nuclear and electronic DOFs, as a function of temperature and proton density.

S1 of the SM reporting electron vs. proton densities).

In the case of the $^{134}_{55}\text{Cs} \rightarrow ^{134}_{56}\text{Ba}$ allowed ($\Delta\pi = \text{no}$, $\Delta J = 0$) transition, the lepton field carries no orbital angular momentum and the rate has been assessed under the assumption, derived by using the nuclear shell model, that the decaying neutron within the parent ^{134}Cs nucleus occupies the $2d_{3/2}$ shell, while the generated proton populates the $1g_{7/2}$ orbital of ^{134}Ba . In our calculations we included the 4^+ GS and the two lowest energy nuclear

states ($5^+, 3^+$, respectively) of ^{134}Cs , occupied according to a Boltzmann distribution $f(E_i) = w_i e^{-E_i/K_B T}$, where E_i is the energy of the i -th nuclear level, weighted by the relevant level degeneration factor ($w_i = 9, 11, 7$, respectively). Our rate has been renormalized at all temperatures by a constant factor, obtained so as to recover the experimental $\log(ft)$ at Earth conditions. This renormalization factor is needed essentially to correct the hadronic current, which may suffer from the WS mean-field evalu-

Table I. Comparison between ^{134}Cs rates obtained using our model and by TY [2] (units in $s^{-1} \times 10^{-8}$).

T_8^a	TY ^b	This work ^b
0.5 (4.31)	1.02	1.02
1 (8.62)	3.28	1.01
2 (17.23)	63.1	2.28
3 (25.85)	211.0	4.73
4 (34.47)	481.0	7.22
5 (43.09)	889.0	9.36

^a $T_8 = 10^8$ K (corresponding values in keV in parentheses).

^b $n_p = 10^{26} \text{ cm}^{-3}$

ation of the nucleon wavefunctions. The electronic DOF is also taken into account.

In Fig. 1a) we compare our results (violet line) with the data set obtained by Takahashi and Yokoi (TY) (green line) [1, 2]. Values obtained with our model compared to TY's results are reported in Table I and in the inset of Fig. 1a); a finer grid of points can be found in Tab. S2 of SM. We stress that in TY's study the effect of the excited nuclear dynamics on the β decay rates was estimated via the $\log(ft)$ values for general β transitions of given forbiddance, typically derived from systematics, as experimental measurements are still unattainable in astrophysical conditions [6, 7]. At odds with our calculations, neither TY include in their estimate the electronic DOF, nor they calculate the nuclear matrix elements from first-principles.

We observe that the inclusion of the nuclear excited state dynamics represents the most relevant effect on the ^{134}Cs β decay rate and is crucial at high temperatures (> 10 keV), where nuclear states are most likely populated. Indeed, the presence of fast-decaying nuclear excited states can increase the rate by a factor of 15 at 100 keV (1 GK) and up to 23 at 1000 keV, with respect to room temperature conditions. In particular, there the half-life decrease can be almost entirely attributed to the 3^+ nuclear excited state, which implies a rate $\simeq 80$ times higher than the 4^+ nuclear GS (if they were at each time the only occupied nuclear states to decay), while GS-only decay increases with temperature (black line in Fig. 1a). We also notice that temperature has a relevant effect on the lepton DOF in the range [0-10] keV (see the difference between the half-life including both DOF (violet line) and with electrons clamped in their GS (cyan line)). In the limit case of a bare nucleus (red curve in Fig. 1a), where all Cs electrons are stripped out (Cs $1s$ binding

energy is $\simeq 36$ keV), the half-life is consistently lower (by 20% in laboratory conditions) than the one of the neutral atom, as the emitted β -electron can land in any bound orbital. Finally, we stress that our half-lives differ from those obtained by using the centroid of the $\log ft$ general systematics, which include all β transitions of all the elements for a given forbiddance. In Fig. 1a) we report the reference band of ^{134}Cs half-life using the standard deviation (centroid $\pm\sigma$, yellow and orange lines, respectively) of such systematics. We notice that TY's recommendations are however out of this range. Our results (cyan line), at variance, are in better agreement with the specific systematics of ^{134}Cs (blue line), where the electronic DOF are of course neglected. Finally, in Fig. 1c) we plot the ^{134}Cs half-life vs. the proton density and temperature varying in the interior of stars. We notice that, at temperatures > 10 keV, the half-life shows a significant drop, also at very high density, owing to the decay from the ^{134}Cs nuclear excited states.

A similar analysis has been carried out also for the ^{135}Cs β decay. The results obtained with our model are compared with those by TY in Table II (a finer grid can be found in Table S3 of SM and in the inset of Fig. 1b). In Fig. 1b) we also plot the half-life vs. temperature obtained by our DHF model (violet line) with the previous estimate by TY (green line). In this case, both data are found within the range spanned by the general systematics for these transitions (orange and yellow lines showing the maximum and minimum of $\log(ft)$). Again, in cyan we plot the half-life obtained by clamping the electrons in their GS, to determine the electronic contribution to the β transition with increasing temperature. The latter is neglected in TY, while the inclusion of this DOF almost halves the half-life around 10 keV. In Fig. 1d) we plot the half-life vs. temperature and proton density, finding similar, but steeper descent with increasing temperature with respect to ^{134}Cs .

Our results immediately touch recent suggestions [20], according to which a more accurate treatment of β decays in hot plasmas is needed for improving the modelling of Ba isotopes in AGB stars. This is especially true for the composition of presolar SiC grains [5]. Postponing a thorough discussion to a future work, we shall therefore use our rates to revise calculations on that issue [5].

In Fig. 2 (left panel) we present the results obtained by using cross sections from the *Kadonis 1.0* repository [19] and decay rates from TY [5]. The right panel shows the changes obtained exclusively by adopting the β^- decay rates of this work. We stress that the new model curves, reproducing the expectations of AGB stars characterized

Table II. Comparison between ^{135}Cs rates obtained using our model and by TY [2] (units in s^{-1}).

T_8^a	TY ^b	This work ^b	TY ^c	This work ^c	TY ^d	This work ^d	TY ^e	This work ^e
0.5 (4.31)	8.12e-15	1.05e-14	7.90e-15	1.02e-14	7.92e-15	9.70e-15	7.39e-15	9.11e-15
1 (8.62)	1.04e-14	1.44e-14	8.78e-15	1.22e-14	8.04e-15	1.08e-14	7.81e-15	9.79e-15
2 (17.23)	6.91e-13	3.39e-13	6.65e-13	3.27e-13	6.09e-13	3.01e-13	5.52e-13	2.66e-13
3 (25.85)	8.64e-11	4.08e-11	8.55e-11	4.04e-11	8.24e-11	3.91e-11	7.74e-11	3.64e-11
4 (34.47)	9.77e-10	4.66e-10	9.65e-10	4.64e-10	9.52e-10	4.57e-10	9.17e-10	4.38e-10
5 (43.09)	4.18e-09	2.05e-09	4.15e-09	2.05e-09	4.08e-09	2.03e-09	3.96e-09	1.97e-09

^a $T_8 = 10^8$ K (corresponding values in keV in parentheses).

^b $n_p = 10^{26} \text{ cm}^{-3}$

^c $n_p = 3 \times 10^{26} \text{ cm}^{-3}$

^d $n_p = 10^{27} \text{ cm}^{-3}$

^e $n_p = 3 \times 10^{27} \text{ cm}^{-3}$

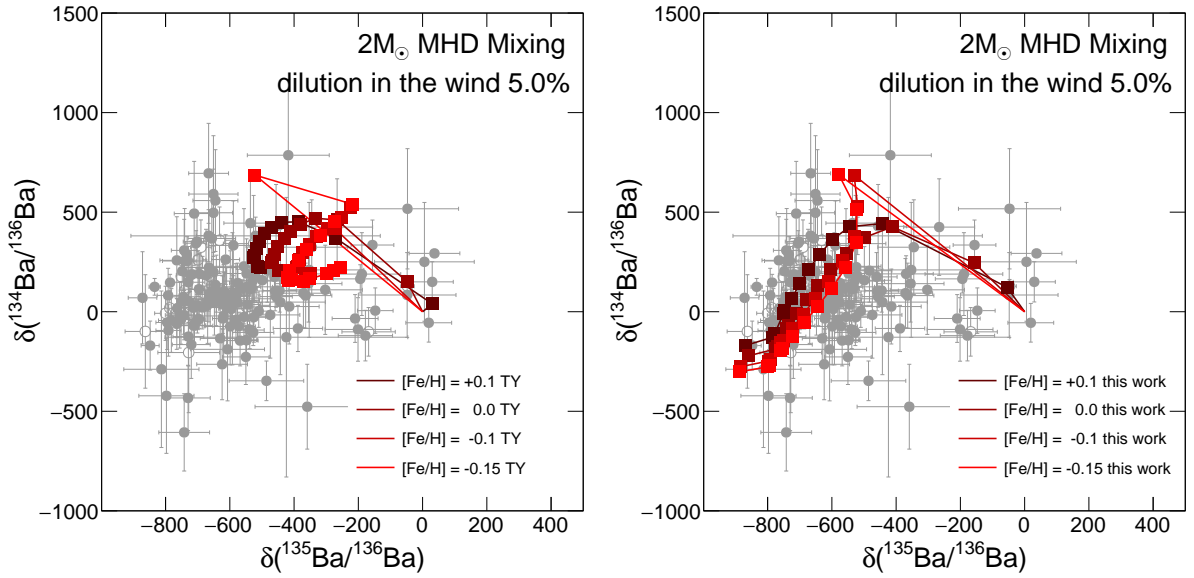


Figure 2. Left panel: the isotopic ratios of ^{134}Ba and ^{135}Ba with respect to ^{136}Ba , displayed as part-per-mil deviations (indicated by the symbol δ), as computed in recent AGB models by [5]. Model curves from stellar masses and metallicities as indicated are from the *standard* case discussed there, with cross sections from [19] and decay rates from TY. Right panel: the results of the same models, where only the decay rates for ^{134}Cs and ^{135}Cs have been changed, using the ones of the present work.

by masses and metallicities as indicated, improve remarkably the agreement with laboratory measurements (gray dots) and fit well the main area occupied by the data. We notice that the novel rates presented here improve even on a tentative guess reported in [5] (see Figure 19(a) therein). A further implication of our half-life revision concerning the solar distribution of s -elements is reported in SM.

In conclusion, we find that the β decay rate of Cs iso-

topes is dramatically increased by two concurrent factors: the inclusion of nuclear and electronic excited states of parent and daughter nuclei, up to complete ionization. Most notably we find i) that the highest energy nuclear excited state of ^{134}Cs at 60 keV, while scarcely populated, is the fastest to β decay, with a rate $\simeq 80$ times higher than the GS-to-GS one; ii) a general increase of the rate with respect to the GS decay only; it is close

to a factor of $\simeq 3$ at 20 keV, $\simeq 6$ at 30 keV, $\simeq 8$ at 40 keV, which are the typical energies characterizing thermal pulses in AGB stars. For ^{135}Cs , where similar concurrent effects of nuclear and electronic DOF in lowering the half-life upon population were found, our results are within the standard deviation of the general systematics. Finally, we stress that the application of our findings to *s*-process computations in AGB stars permits a remarkably improved agreement between models and observations, especially for the presolar SiC grain isotopic composition.

* Correspondence email address: taioli@ectstar.eu

† Correspondence email: stefano.simonucci@unicam.it

- [1] K. Takahashi and K. Yokoi, *Nuclear Physics A* **404**, 578 (1983).
- [2] K. Takahashi and K. Yokoi, *Atomic Data and Nuclear Data Tables* **36**, 375 (1987).
- [3] E. Zinner, in *Treatise on Geochemistry (Second Edition)*, edited by H. D. Holland and K. K. Turekian (Elsevier, Oxford, 2014) second edition ed., pp. 181 – 213.
- [4] N. Liu, T. Stephan, P. Boehnke, L. R. Nittler, B. S. Meyer, C. M. O. Alexander, J. Wang, R. Trappitsch, M. J. Pellin, and A. M. Davis, in *80th Annual Meeting of the Meteoritical Society*, Vol. 80 (2017) p. 6283.
- [5] S. Palmerini, M. Busso, D. Vescovi, E. Naselli, A. Piatella, R. Mucciola, S. Cristallo, D. Mascalì, A. Mengoni, S. Simonucci, and S. Taioli, in press (2021), arXiv:2107.12037 [astro-ph.SR].
- [6] D. Mascalì, A. Musumarra, F. Leone, F. P. Romano, A. Galatà, S. Gammino, and C. Massimi, *The European Physical Journal A* **53**, 145 (2017).
- [7] D. Mascalì et al., *EPJ Web Conf.* **227**, 01013 (2020).
- [8] K. Nomoto, C. Kobayashi, and N. Tominaga, *Annual Review of Astronomy and Astrophysics* **51**, 457 (2013).
- [9] S. Simonucci, S. Taioli, S. Palmerini, and M. Busso, *The Astrophysical Journal* **764**, 118 (2013).
- [10] D. Vescovi, L. Piersanti, S. Cristallo, M. Busso, F. Visani, S. Palmerini, S. Simonucci, and S. Taioli, *Astronomy & Astrophysics* **623**, 7 (2019).
- [11] A. Sonzogni, *Nuclear Data Sheets* **103**, 1 (2004).
- [12] S. Palmerini, M. Busso, S. Simonucci, and S. Taioli, *Journal of Physics: Conference Series* **665**, 012014 (2016).
- [13] B. Singh, A. A. Rodionov, and Y. L. Khazov, *Nuclear Data Sheets* **109**, 517 (2008).
- [14] T. Morresi, S. Taioli, and S. Simonucci, *Advanced Theory and Simulations* **1**, 1870030 (2018).
- [15] L. Hayen, N. Severijns, K. Bodek, D. Rozpedzik, and X. Mougeot, *Rev. Mod. Phys.* **90**, 015008 (2018).
- [16] M. Hjorth-Jensen, M. P. Lombardo, and U. van Kolck, eds., *An advanced course in computational nuclear physics: Bridging the scales from quarks to neutron stars*, Lecture notes in physics, Vol. 936 (Springer, Cham, 2017) p. 644 pages.
- [17] J. C. Slater, *Phys. Rev.* **81**, 385 (1951).
- [18] F. Salvat, J. D. Martinez, R. Mayol, and J. Parellada, *Phys. Rev. A* **36**, 467 (1987).
- [19] I. Dillmann, T. Szücs, R. Plag, Z. Fülöp, F. Käppeler, A. Mengoni, and T. Rauscher, *Nuclear Data Sheets* **120**, 171 (2014), arXiv:1408.3688 [astro-ph.SR].
- [20] M. Busso, D. Vescovi, S. Palmerini, S. Cristallo, and V. Antonuccio-Delogu, *Astrophys. J.* **908**, 55 (2021).
- [21] N. Schwierz, I. Wiedenhover, and A. Volya, arXiv:0709.3525 [nucl-th] (2007).
- [22] M. R. Harston and N. C. Pyper, *Phys. Rev. A* **45**, 6282 (1992).
- [23] N. Prantzos, C. Abia, S. Cristallo, M. Limongi, and A. Chieffi, *Monthly Notices of the Royal Astronomical Society* **491**, 1832 (2020).

Supplemental Material: Theoretical estimate of the half-life for the radioactive ^{134}Cs and ^{135}Cs in astrophysical scenarios

THEORETICAL AND COMPUTATIONAL MODEL

Here we recap few mathematical and computational details of our method for calculating β decay in astrophysical scenarios. In the traditional approach, β decay spectra of allowed and forbidden transitions are calculated by using an analytical expression of the rate [15] where several factors appear, which account for the nuclear and phase-space structure, and for the atomic exchange.

At variance, our approach is based on the calculation of the total Hamiltonian of the system:

$$\mathcal{H} = \mathcal{H}_{\text{nuc}} + \mathcal{H}_{\text{e-e}} + \mathcal{H}_{\text{weak}}, \quad (1)$$

where \mathcal{H}_{nuc} contains the interactions between nucleons in the initial and final nuclear states, $\mathcal{H}_{\text{e-e}}$ is the electron-electron Coulomb correlation, taking into account that the transition occurs inside a partially ionized atom, and finally $\mathcal{H}_{\text{weak}}$ is the zero-order QED weak interaction, which fulfills the Lorentz-invariance:

$$\mathcal{H}_{\text{weak}} = \frac{G_F}{\sqrt{2}} H_\mu L^\mu + \text{h.c.}, \quad (2)$$

where $G_F = 1.16637 \times 10^{-5} \text{GeV}^{-2}$, L^μ is the lepton current:

$$L^\mu = \bar{u}_e \gamma^\mu (1 - \gamma^5) v_\nu, \quad (3)$$

and H_μ is the hadronic current:

$$H_\mu = \bar{u}_p \gamma_\mu (1 - x \gamma^5) v_n \quad (4)$$

In Eqs. (3,4) $\gamma^\mu, \mu = 0, \dots, 4$ are the Dirac matrices, and u_e, v_ν, v_n, u_p are the β -electron, neutrino, neutron and proton annihilation operators, respectively.

In particular, we are interested in reckoning the probability per unit time that the atomic system decays from a statistical mixture of initial states $\hat{\rho}_i = p_i |i\rangle \langle i|$ to a mixture of final states $P_f = \sum_f |f\rangle \langle f|$, that is:

$$N_{i \rightarrow f} = 2\pi \text{Tr}(\hat{\rho}_i \mathcal{H}_{\text{weak}} P_f \mathcal{H}_{\text{weak}}) \delta(E_i - E_f) + \text{h.c.} \quad (5)$$

In the typical approximation to the general theory of β decay, where the recoil energy of the final nucleus is small with respect to the nucleon rest mass, the initial and final states can be written as:

$$|i\rangle = |h_i\rangle \otimes |e_i\rangle \quad (6)$$

$$|f\rangle = |h_f\rangle \otimes |e_f\rangle \otimes |\bar{\nu}_f\rangle \quad (7)$$

where $|h_{(i,f)}\rangle$ are initial and final multi-nucleon states characterized by the quantum numbers $|J_{(i,f)}, M_{(i,f)}, T_{(i,f)}\rangle_{\text{nuc}}$, where $J_{(i,f)}, M_{(i,f)}$ denote the total angular momentum and its projection along some fixed axis of the initial and final states, respectively, and $T_{(i,f)}$ is the isospin; $|e_i\rangle = |j_i, m_i; [n_1^b \dots n_k^b]_{(i)}\rangle_{\text{e-e}}$ is the initial many-electron state, where $[n_1^b \dots n_k^b]_{(i)}$ represent the bound orbitals; finally, $|\bar{\nu}_f\rangle$ is the final anti-neutrino state (typically represented by a free plane wave). We point out that the initial and final multi-nucleon states and the initial multi-electron states are characterized by a discrete spectrum, while the final multi-electron state, which describes the β emission, is a continuum state that can be written as a linear combination of external products $|e_f\rangle = \sum_j I_{j,f} \wedge |\eta_{j,f}\rangle$, where $|\eta_{j,f}\rangle$ describes the β -electron continuum wavefunction and $I_{j,f}$ represents the final bound state.

Within this framework, the evaluation of the transition operator can be factorized into the product of lepton and hadronic currents [14]. This is ultimately due to the large rest mass of the W vector boson that mediates the weak

interaction. Furthermore, we can safely assume that electrons and neutrinos are not coupled and thus the lepton current (3) can be further factorized in the independent product of the neutrino and electron quantum field operators (or, dealing with expectation values, wavefunctions). In this work, we also make the assumption that the hadronic current can be factorized in the product of neutron and proton field operators. The hadronic current separability is basically equivalent to require that only one nucleon within the parent nucleus participates into the decay dynamics. The decaying nucleon is thus an independent particle, uncorrelated to the “core” of the remaining nucleons. Such a core, which couples only geometrically to the decaying nucleon so as to recover the total angular momentum of the parent reactant and of the final daughter nucleus, is approximated by a linear combination of angular momentum wavefunctions. Our approximation assumes the validity of the nuclear shell model. However, this does not represent an intrinsic limit of our method, as the hadronic current for systems where many-body effects are expected to play a paramount role can be assessed separately, via more accurate first-principle approaches [16]. The hadronic current (4) is derived by an explicit numerical solution of the Dirac equation (DE) in a central potential. In our solution, protons and neutrons interact via a semi-empirical scalar and vector relativistic Wood-Saxon (WS) spherical symmetric potential, which describes the nucleon-nucleon interaction [21], whereby the DE is mono-dimensional in the radial variable. To solve the equation, a grid with a few thousands points is used [14].

Also the electron wavefunctions are found by solving self-consistently the Dirac-Hartree-Fock (DHF) equation in a central potential. Electrons interact via a mean-field, where the non-local exchange (Fock term) is replaced by the local density approximation (LDA) to the electron gas ($V_{ex} \propto \rho(r)^{1/3}$) [17, 18]. The numerical solution of the DHF equation was found by using a modified Runge-Kutta method [14]. The non-orthogonality between the bound initial n_i^b and final n_f^b orbitals, which are obtained by solving the DHF equations for the parent and daughter nuclei carrying a different atomic number is taken into account. The continuum β -electron wavefunction $\psi_{f,e}^c(\mathbf{r})$ is then expressed in the field produced by both the nucleus and the surrounding electrons as a Slater determinant, to take into account the atomic exchange. The β -electron continuum wavefunction within this framework thus reflects the fact that the emitted lepton may decay into a bound state of the daughter nucleus with ejection of a secondary bound electron and that final state excitations, such as shake-up and shake-off [14], can be present. Atomic exchange effects open up multiple decay channels that typically increase the β decay rate particularly at low energies [22], where the overlap between the continuum and discrete wave functions maximizes.

Electrons populate the energy levels according to a Fermi-Dirac (FD) distribution $n_{e-}^i = \frac{1}{1+e^{(\epsilon_i - \mu_{e-})/(K_B T)}} = F(T, \mu_{e-})$, where K_B is the Boltzmann constant and T is the temperature. The eigenvalues ϵ_i are obtained by a self-consistent solution of the DHF equation for the leptons, and the chemical potential is assessed by assuming that the electrons behave as an ideal Fermi gas in a box with a relativistic energy-momentum dispersion $E^2 = c^2 p^2 + m_e^2 c^4$

Table S1. n_e/n_p and $(n_e - n_p)/n_p$ ratios of proton densities $n_p = 10^{26}$ and $n_p = 10^{27}$ (cm^{-3}) and of the resulting electron densities n_e as a function of temperatures T (keV).

T	$n_p = 10^{26}$		$n_p = 10^{27}$	
	n_e/n_p	$(n_e - n_p)/n_p$	n_e/n_p	$(n_e - n_p)/n_p$
10	1.0	0.0	1.0	0.0
20	1.0	2.121e-18	1.0	2.234e-21
30	1.0	2.381e-10	1.0	2.57342e-13
40	1.0	2.5098e-06	1.0	2.74123e-09
50	1.0009	0.00087	1.0	9.5167e-07
60	1.0460	0.0460	1.00005	5.3074e-05
70	1.5858	0.5858	1.001025	0.001025
80	3.5663	2.5663	1.010026	0.010026
90	8.0831	7.0831	1.0599	0.05987
100	16.61334	15.61334	1.2334	0.2333676

as $n_{e-} = \int_0^\infty dp p^2/\pi^2 \times (F((c \times \sqrt{p^2 + m_e^2 c^2}) - \mu_e)/K_B T) - F((c \times \sqrt{p^2 + m_e^2 c^2}) + \mu_e)/K_B T)$. We notice that the electron orbitals of Cs and Ba have not been re-optimized at each temperature. At very high temperature, however, we included positron formation in our model. The plasma at a given temperature is assumed overall neutral, that is $n_p = n_{e-} - n_{e+}$, where n_p, n_{e-}, n_{e+} are the proton, electron, and positron density, respectively. Note that $n_p \approx n_{e-}$ at high densities, while they can differ sensibly at low densities. Protons are treated as nonrelativistic particles and their density has been varied in the range $n_p = 10^{24} - 10^{27}$ to model different astrophysical scenarios. In Table S1 we report the proton vs. relevant electron densities at different temperatures.

HAL-LIFE TABLES

Here we report the half-lives of both ^{134}Cs and ^{135}Cs on a finer mesh.

Table S2. ^{134}Cs half-lives (years) obtained by our model for several densities (cm^{-3}) and temperatures T (keV).

T	n_p					
	6e+24	6e+25	6e+26	6e+27	6e+28	6e+29
0.86	2.04149	2.05406	2.07755	2.15924	2.55484	5.56986
1.085	2.03336	2.05026	2.07621	2.15899	2.5548	5.56984
1.37	2.01435	2.04481	2.07446	2.15896	2.55518	5.57079
1.719	1.9947	2.03652	2.07328	2.16047	2.55763	5.57629
2.16	1.98896	2.02753	2.07546	2.16711	2.56659	5.59606
2.725	2.00225	2.02915	2.08667	2.18582	2.59062	5.64877
3.43	2.03635	2.05478	2.11409	2.2243	2.63937	5.75549
4.319	2.07298	2.10883	2.16471	2.2886	2.72088	5.93362
5.44	2.00961	2.17161	2.23866	2.37687	2.83378	6.1752
6.845	1.86683	2.1586	2.30543	2.46085	2.94249	6.35983
8.62	1.78273	1.97719	2.24599	2.43095	2.90337	6.01333
10.85	1.58026	1.64867	1.87921	2.08555	2.4593	4.55354
13.66	1.17738	1.19422	1.29305	1.45373	1.67893	2.70035
17.19	0.765335	0.769108	0.798542	0.886004	1.00964	1.47377
21.65	0.48386	0.484805	0.493239	0.533676	0.606594	0.84334
27.25	0.321219	0.321509	0.324257	0.342418	0.389374	0.530591
34.31	0.228839	0.228947	0.229995	0.238386	0.269924	0.365959
43.19	0.174786	0.174833	0.175296	0.179417	0.200815	0.27283
54.37	0.141613	0.141634	0.141865	0.144038	0.158478	0.215895
68.453	0.120307	0.120315	0.120432	0.121659	0.131326	0.178361
86.17	0.106109	0.106113	0.106165	0.106871	0.113322	0.151812

Table S3. ^{135}Cs half-lives (years) obtained by our model for several densities (cm^{-3}) and temperatures T (keV).

T	n_p					
	6e+24	6e+25	6e+26	6e+27	6e+28	6e+29
0.86	2.24735e+06	2.28314e+06	2.35169e+06	2.5949e+06	4.05442e+06	1.38295e+08
1.085	2.22363e+06	2.27205e+06	2.34741e+06	2.59384e+06	4.05376e+06	1.38122e+08
1.37	2.16957e+06	2.25504e+06	2.3407e+06	2.59214e+06	4.05272e+06	1.37847e+08
1.719	2.11206e+06	2.22521e+06	2.33048e+06	2.58945e+06	4.05111e+06	1.37424e+0
2.16	2.07881e+06	2.17983e+06	2.31431e+06	2.58509e+06	4.04856e+06	1.36759e+08
2.725	2.06411e+06	2.1325e+06	2.28881e+06	2.57781e+06	4.04444e+06	1.35701e+08
3.43	2.0522e+06	2.09846e+06	2.25322e+06	2.56603e+06	4.03796e+06	1.34072e+08
4.319	1.97606e+06	2.07086e+06	2.21036e+06	2.54721e+06	4.02766e+06	1.3157e+08
5.44	1.62748e+06	1.9987e+06	2.16292e+06	2.51833e+06	4.01129e+06	1.27794e+08
6.845	1.24302e+06	1.75501e+06	2.09403e+06	2.47574e+06	3.9854e+06	1.22285e+08
8.62	1.10909e+06	1.39724e+06	1.94529e+06	2.41137e+06	3.94404e+06	1.14477e+08
10.85	1.07248e+06	1.18395e+06	1.67416e+06	2.29764e+06	3.85507e+06	9.81098e+07
13.66	806399	834310	1.02279e+06	1.44121e+06	2.24393e+06	1.27362e+07
17.19	72041.5	72659.3	77637.2	94275.4	123468	340712
21.65	3851.17	3865.52	3995.78	4683.27	6254.44	16801.2
27.25	358.829	359.506	365.995	412.098	563.022	1513.15
34.31	53.6033	53.6588	54.2028	58.7768	80.1084	214.686
43.19	11.6125	11.6195	11.6889	12.3265	16.2948	42.9303
54.37	3.34727	3.34841	3.36067	3.47855	4.37922	11.0515
68.453	1.20894	1.20911	1.2117	1.23923	1.47913	3.46087
86.17	0.527193	0.527237	0.527765	0.535284	0.609228	1.28288

THE IMPACT OF OUR RATE ON s -PROCESSES

Here we show one further implication of our half-life revision by performing some of the calculations carried out in Refs. [5, 20]. In particular, very recently rather extensive analyses of neutron captures in AGB stars pointed out how a reappraisal of the rates here presented for β^- decays, with a more accurate treatment of their dependence on temperature and density, was crucial for any improvement in our understanding of the isotopic admixture of Ba in the Sun [20]. In particular, it was shown that (see Fig. 4 in [20]) an *average* model could be identified, suitable to mimic (if properly normalized) the outcomes of a simulation from a chemical evolution model of the Galaxy at least for the s -process contribution to heavy nuclei. In those estimates, ^{134}Ba and ^{136}Ba should be both at the level of one (as they do not receive contributions from other processes). In Fig. S1 we show the results of the calculations carried out using the same physical models and nuclear parameters as in Ref. [20], only updating the two rates discussed here. With blue dots we show the original results for s -only nuclei sited close to the *magic* neutron number $N = 82$. In red we report the new values found for ^{134}Ba and ^{136}Ba using our new rates (all the rest remaining untouched). We stress that the improvement over the previous expectations is striking. We notice that similar improvements are also expected for Galactic Chemical Evolution models computed with full stellar evolutionary yields [23], which were showed to have severe problems with ^{134}Ba and ^{136}Ba .

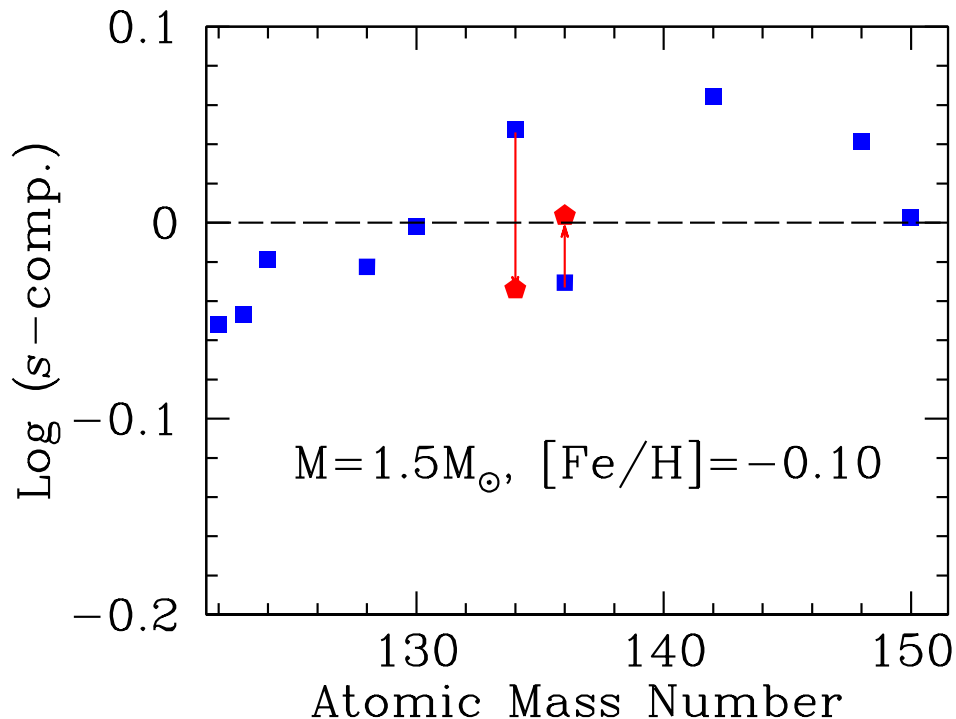


Figure S1. Percentage of s -process contributions (blue dots) as computed by [20], for s -only nuclei near the magic neutron number $N = 82$. In a perfect model, without nuclear or stellar uncertainties, all points should be aligned at zero. Red points (marked by arrows) show the results for ^{134}Ba and ^{136}Ba in a revised calculation where, all the rest remaining the same, we adopted the β^- -decay rates for ^{134}Cs and ^{135}Cs computed in the present work. We note that two more nuclei look as outliers in the figure. They are ^{142}Nd and ^{148}Sm , whose abundances are critically linked to the decay rates of ^{142}Pr , ^{147}Nd and ^{148}Pm , for which a revision like the present one would be needed.